

STUDY COHORTS: For external validation of models, we tested them in an independent cohort of 147 patients treated with R-CHOP (DLBCL4), using diagnostic specimens from patients treated at the British Columbia Cancer Agency (n=64), Stanford University Medical Center (n=49), University of Miami Cancer Center (n=23), and Hospital Santa Creu i Sant Pau in Barcelona (n=11). Cases were selected based on: (1) diagnosis of *de novo* DLBCL of any clinical stage; (2) availability of tissue obtained at diagnosis prior to therapy; (3) treatment with curative intent with R-CHOP (DLBCL1 and DLBCL4) or CHOP (DLBCL2 and DLBCL3); and (4) availability of outcome data at the treating institution. Criteria commonly used for prospective trial enrollment such as normal renal and liver functions, absence of co-morbid conditions, and good performance status were not applied for case selection. Patients with primary mediastinal large B-cell lymphoma or central nervous system involvement at presentation were excluded. Follow-up information was obtained from the patients' medical records and included response to initial therapy based on the Cheson criteria,¹ and the clinical endpoints analyzed included overall (OS), and progression free (PFS), with data censored for patients who did not have an event at the last follow-up visit. Histological sections were reviewed to confirm the diagnoses based on features of DLBCL according to the World Health Organization classification.²

MICROARRAY DATA: Gene expression data for 414 adult patients with DLBCL, treated with R-CHOP (n=233; DLBCL1) or CHOP (n=181; DLBCL2), and profiled with Affymetrix HG-U133 Plus 2.0 microarrays by Lenz *et al*³ and the LLMP, were obtained from the NCBI Gene Expression Omnibus (GSE10846). Outcome data and the corresponding clinical information were kindly provided by the authors.

A set of 131 patients with DLBCL and treated primarily with CHOP-based regimen and profiled with Affymetrix HG-U133A microarrays by Hummel *et al*.⁴ was used as an additional test cohort (DLBCL3) for the TGS (IPI was not available); expression data were obtained from NCBI GEO (GSE4475). Within DLBCL3, we excluded Burkitt Lymphoma (BL) cases by selecting only cases that had p<0.05 for predicted

molecular classification as BL as defined by the authors, leaving 131 patients with DLBCL among whom 96 had survival data.

We used two tailed t-tests and analysis of variance for the estimation of significant differences in gene expression level across cancer types profiled as part of the Expression Project for Oncology (*expO*) (<http://www.intgen.org/expo/>), obtained from NCBI GEO as GSE2109.

For DLBCL expression profiles, probe set summaries were derived from Affymetrix microarray data from raw CEL files using a custom Chip Definition File (CDF) mapping to Entrez Gene identifiers (version 12).⁵ Data were normalized with MAS5, with intensities scaled to a global median of 500 for each array. Base-2 logarithms of normalized measurements were employed in estimating mRNA expression levels for *LMO2* and *TNFRSF9*, and for corresponding statistical measures for associations with cell-of-origin, International Prognostic Index, and outcomes including OS.

STATISTICAL METHODS: In constructing the final model comprising *LMO2* and *TNFRSF9*, expression values across the microarray datasets were centered and scaled to match PCR validation data (detailed below). This avoids the necessity to apply corrective factors to future prospectively gathered patient sample measurements. The *two-gene score* (TGS) was computed in the test sets (DLBCL2, 3, and 4) using the same weighting parameters derived in the training cohort (DLBCL1). The thresholds for separating the training cohort into risk groups were directly applied to the validation sets. The resulting scores were tested as univariate predictors of outcome, and in multivariate combination with other variables. Within cell-of-origin subtypes, we tested for ability of TGS to distinguish the High Risk group from the others for GCB-Like cases, and the Low Risk group from the others in ABC-Like cases in discrete fashion (log-rank test), as well as testing TGS as a continuous variable (Cox log-likelihood test). Continuous risk score curves were generated using the *coxph* function in the R software package, estimating the baseline using the Breslow method. Resulting confidence intervals for survival at each time were smoothed using cubic splines.

To obtain a composite model (i.e., the TGS-IPI) incorporating *LMO2*, *TNFRSF9*, and IPI, we applied multivariate Cox regression to the training set, with the independent variables being the previously computed TGS, together with the traditional IPI score of each patient (on a scale ranging from 0 to 5). Thus, the relative weights of *LMO2* and *TNFRSF9* were not changed in the composite TGS-IPI model when compared with the TGS. A constant (4) was added as a term within the TGS-IPI to avoid negative scores, based on the lowest non-adjusted measurement observed across studies. For a minority of patients in the training cohort, evaluation of all IPI risk factors was not available, where it invariably related to patients missing only one of the five component risk factors. In those cases, we did not employ imputation and instead used the average of the minimum and maximum possible IPI score defined by available factors. The validation cohort had no missing data for components of the TGS, IPI, OS, or PFS. As with the TGS, the TGS-IPI was also computed in the test sets using the same parameters derived in the training cohort (DLBCL1). The resulting scores were tested as univariate predictors of outcome, and in multivariate combination with other variables.

Alternate versions of the TGS with equal weightings of *LMO2* and *TNFRSF9* (i.e., $TGS = LMO2 - TNFRSF9$) and the TGS-IPI ($TGS-IPI = 2 \times IPI - LMO2 - TNFRSF9$) yielded nearly identical results within test and validation cohorts, suggesting that the simplicity of these equations might promote their clinical adoption in the manner of the IPI. However, we opted to keep the weightings in the final models of TGS and TGS-IPI, since the quantitative measurements of the two genes are likely to require arithmetic that is unlikely to be done at the bedside. To facilitate calculation of the risk scores and corresponding risk groups based on the described thresholds for the TGS, IPI, and TGS-IPI, we devised an online calculator, publicly available at <http://tgs.stanford.edu>.

Table S1. *LMO2* expression retains prognostic value in DLBCL when considering it alongside the germinal center signature, as covariates in a multivariate model for overall survival after R-CHOP chemotherapy (DLBCL1 dataset, as specified within Table 1).

Overall Survival, Covariate	HR (95% CI)	P
<i>LMO2</i> expression	0.8 (0.6-0.9)	0.009
Germinal Center Signature	0.7 (0.5-1.1)	0.15
Overall		<0.0001

Table S2. *TNFRSF9* as best univariate and bivariate predictor among genes more highly expressed in non-tumor cells. Bivariate combinations of genes with *LMO2* were tested for their ability to predict survival using multivariate Cox regression, limited to genes with higher expression among non-tumor cells (CD19-) as compared with paired t-test ($p < 0.05$) to matched tumors cells (CD19+), and exhibiting significant ($p < 0.01$) univariate predictive value in R-CHOP treated patients (DLBCL1). Within this group of genes, *TNFRSF9* was best as a univariate predictor and also as a bivariate partner for *LMO2*. The top 15 genes are shown, ranked by p-value of the bivariate model.

Entrez Gene Identifier	Gene Symbol	Association with overall survival in RCHOP training cohort (DLBCL1)			Tumor vs. Micro-Environment (CD19+ vs CD19-)
		Univariate		Bivariate (with <i>LMO2</i>)	p-value (paired T-test)
		z-score	p-value	p-value	
3604	<i>TNFRSF9 (CD137)</i>	-4.30	1.72E-05	2.33E-08	0.04
5578	<i>PRKCA</i>	-3.21	1.32E-03	1.04E-07	0.01
5334	<i>PLCL1</i>	-3.22	1.29E-03	1.67E-07	0.01
64375	<i>IKZF4</i>	-3.71	2.09E-04	1.93E-07	0.04
80273	<i>GRPEL1</i>	3.23	1.24E-03	1.06E-06	0.00
81615	<i>TMEM163</i>	-3.09	2.03E-03	1.17E-06	0.02
56548	<i>CHST7</i>	3.80	1.44E-04	1.46E-06	0.04
113763	<i>C7orf29</i>	-3.15	1.61E-03	1.65E-06	0.00
321	<i>APBA2</i>	-3.05	2.26E-03	1.74E-06	0.05
3687	<i>ITGAX</i>	-3.70	2.20E-04	2.33E-06	0.01
286133	<i>SCARA5</i>	-2.60	9.36E-03	3.65E-06	0.05
5919	<i>RARRES2</i>	-2.74	6.07E-03	4.58E-06	0.01
2060	<i>EPS15</i>	-3.22	1.29E-03	5.04E-06	0.03
6355	<i>CCL8</i>	2.76	5.74E-03	6.25E-06	0.01
4208	<i>MEF2C</i>	-2.75	5.92E-03	1.45E-05	0.01

Table S3. Multivariate analysis of overall survival after R-CHOP therapy (DLBCL1 microarray dataset). In a multivariate model considering IPI, TGS, and Stromal score (comprising the Germinal center signature, Stromal1 and Stromal2 signatures), only the IPI and TGS remain significant predictors of OS.

Overall Survival, Covariates	H.R. (95% CI)	P
IPI Score (0-5)	1.8 (1.4-2.2)	<0.0001
Two Gene Risk Score (TGS)	2.3 (1.4-3.8)	0.001
Stromal Score (381 genes)	1.1 (0.7-2.0)	0.59
Overall		<0.0001

Table S4: In a multivariate analysis for outcomes after R-CHOP therapy within the external validation cohort (DLBCL4 dataset), both TGS and IPI remain as independent predictors of OS and PFS.

Covariate	Overall Survival		Progression Free Survival	
	HR (95% CI)	P	HR (95% CI)	P
Two Gene Risk Score (TGS)	1.9 (1.2-3.1)	0.006	2.2 (1.4-3.4)	0.0003
IPI Score (0-5)	2.2 (1.7-3.0)	<0.0001	1.8 (1.4-2.4)	<0.0001
Overall		<0.0001		<0.0001

Figure S1. *LMO2* expression has prognostic utility in different therapeutic eras, independently of DLBCL subtype. Panel A depicts univariate associations between genome-wide expression, survival, and therapeutic era. Expression profiles of 17888 genes tested for their association with OS in 414 patients treated with R-CHOP (DLBCL1, y-axis) or CHOP (DLBCL2, x-axis).^{3, 6} Each point depicts a single gene, and saturation of color within the shaded central cloud represents gene density (frequency of genes within a region); single genes occurring in low density regions are indicated by a black point. *LMO2* is among the best univariate predictors considering all measured genes, in both R-CHOP and CHOP treated patients. The position of *TNFRSF9* is also indicated. Genes generally tend to have significant positive correlation in prognostic influence when comparing therapeutic eras (Pearson $r = 0.44$, $p < 2 \times 10^{-16}$). **(B)** *LMO2* expression is correlated (rank correlation = 0.68, $p < 0.0001$) with the Germinal Center Signature.³ **(C)** Receiver-operator curve (ROC) characteristics depict performance of *LMO2* expression as an effective surrogate for cell of origin in independent cohorts. An optimal threshold of *LMO2* expression of 1.85 (depicted by the blue-rimmed white circular marker) was derived within DLBCL1, exhibiting 87% sensitivity and 70% specificity for discrimination of GCB- from ABC-like DLBCL. The corresponding ROC profile had an area under curve of 0.84 (95% CI 0.78-0.88, $p < 0.0001$, binomial exact test using method of DeLong et al.). This same threshold was validated in DLBCL2, where it exhibited 85% sensitivity and 73% specificity. **(D)** Prognostic value of *LMO2* expression is independent of cell-of-origin classification, as it retains prognostic value among GCB-like DLBCL, including multivariate analyses (DLBCL1 dataset, Table 1). Patients were stratified according to *LMO2* expression relative to its median level among GCB-like DLBCL. **Panels E-G:** *LMO2* expression is a strong univariate predictor of outcome after therapy with CHOP or R-CHOP, as depicted by Kaplan Meier strata in 3 cohorts profiled by microarrays; panels E-F correspond to DLBCL1-3, respectively. Depicted strata reflect tertiles of expression of *LMO2* within the

corresponding cohort. For DLBCL3, tertiles were defined across all patients with DLBCL, with a subset having corresponding survival data.

Figure S2. *TNFRSF9* (CD137) expression is a strong univariate predictor of outcome after therapy with CHOP or R-CHOP, as depicted by Kaplan Meier strata in 3 cohorts profiled by microarrays. Panels A, B, and C correspond to DLBCL1, 2, and 3, respectively. Depicted strata reflect tertiles of expression of *TNFRSF9* within the corresponding cohort. For DLBCL3, tertiles were defined across all patients with DLBCL, though only a subset had corresponding survival data.

Figure S3. Relative *TNFRSF9* expression and relation to outcomes in diverse human tumors. (A) *TNFRSF9* is highly expressed in B-cell lymphomas relative to other cancers. Variation in expression of *TNFRSF9* mRNA is depicted in relation to histological classification across 1822 tumor specimens, as profiled within *Expression Project for Oncology (expO)* using microarrays. Vertical bars within boxes reflect median expression level, boxes depict the interquartile range, and whiskers bound 95% confidence intervals with outliers represented by single points. *TNFRSF9* is more highly expressed in lymphomas than in other cancer types ($p < 0.0001$). (B-D) Stratification of outcomes based on level of expression of *TNFRSF9* in patients with adenocarcinomas of the breast (B), colon (C), and lung (D). Panel (B) depicts distant metastasis free survival (DMFS) of a cohort of 286 women previously described (NKI/Rotterdam, GSE2034) as diagnosed with early stage breast adenocarcinomas between 1980-1995 and without lymph node involvement at presentation (Age 26-83, ER+ 73%, PR+ 58%).^{7, 8} Panels C and D depict overall survival (OS) for cohorts of previously described patients as diagnosed with colorectal adenocarcinomas ($n=177$, GSE17536)⁹ and lung adenocarcinomas ($n=179$ [University of Michigan], NCI-caArray: jacob-00182-UM)^{8, 10}, respectively. Depicted strata reflect patients classified as expressing High (red curve), or Low (blue curve) levels of *TNFRSF9* mRNA as measured on HG-U133 series Affymetrix microarrays, with dotted lines representing 95% confidence intervals. High and Low labels relate to an idealized cut-point¹¹ of *TNFRSF9* expression exhibiting strongest association with the depicted outcome,

and meriting consideration after correction for multiple hypothesis testing. After such correction,¹² the two-sided log-rank p-values for the dichotomous stratifications depicted in panels B, C, and D were p=0.005, 0.004, and 0.06, respectively. The corresponding estimates for the association between continuous expression of *TNFRSF9* and as measured by the log-likelihood test within a univariate Cox regression model were p=0.002, 0.006, and 0.04, respectively.

Figure S4. CD137 mRNA and protein expression levels are concordant. CCRF-CEM cells (a T-cell line) were stimulated over a 16-hour time course with ionomycin (10ng/mL) and PMA (500ng/mL) as previously described,¹³ and induced CD137 expression was measured by (A) flow cytometry (FACS), (B) quantitative real-time PCR (qRT-PCR), and (C) immunohistochemistry (IHC). Enumeration of CD137 immunohistochemical staining for 10 high power fields (40X) estimated less than 5% staining among unstimulated cells, with the corresponding estimate after 16 hours of stimulation being 60%. (E) High correlation between mRNA and cell surface expression of *TNFRSF9*/CD137 as measured by qRT-PCR and FACS, respectively.

Figure S5. Distribution of Two Gene Scores (TGS) and relationship to survival. Relationship of the survival model captured by TGS within the training cohort (DLBCL1), as a continuous function of the score. As a continuous variable, the bivariate model was associated with an increase in the relative risk of death of 2.7 (95%CI, 2.0 to 3.8) per unit increment of the score. Tertiles of the TGS define the three risk strata depicted in Figure 3A-C [i.e., High Risk, $TGS > -0.91$; Intermediate Risk, $-0.91 \geq TGS > -1.60$; Low Risk, $TGS \leq -1.60$]; validity of these thresholds in other cohorts was examined in Figures 4 (DLBCL4), S6 (DLBCL2,3), and S9 (DLBCL4). Scores for individual patients are depicted as a 'rug' plot atop the x-axis.

Figure S6. The TGS-IPI is validated in a test cohort treated with CHOP. By applying thresholds derived from tertiles in the R-CHOP treated training cohort, the TGS-IPI also stratifies overall survival of patients in a test cohort treated with CHOP (DLBCL2, p<0.0001 HR=2.0 [1.7-2.5]). IPI data were not available for DLBCL3, precluding a similar analysis.

Figure S7. TGS is independent of the IPI. Kaplan Meier analyses reveal that TGS risk groups can further stratify individual IPI risk categories of patients treated with RCHOP (A,B,C; DLBCL1), or CHOP (D,E,F; DLBCL2), including patients with (A, D) Low (IPI=0,1), (B, E) Intermediate (IPI=2,3), or (C,F) High IPI Risk (IPI=4,5).

Figure S8. The TGS compares favorably to other multi-gene prognostic models. Stratification of overall survival with (A) 2 genes (using the TGS), as compared with the (B) 6-gene model of Lossos et al, and (C) the 381 genes within the Stromal Model of Lenz et al within a cohort of patients treated with R-CHOP (DLBCL1).

Figure S9. *LMO2*, *TNFRSF9*, and the Two Gene Score (TGS) are validated in a simple assay of fixed diagnostic specimens from a cohort treated with R-CHOP. Within the external validation cohort (DLBCL4), expression of *LMO2* (A, B) and *TNFRSF9* (C, D) alone, and their combination as the TGS (E, F), are predictors of overall (A, C, E) and progression free survival (B, D, F). Continuous expression levels of *LMO2*, *TNFRSF9* were individually significant as predictors of OS and PFS, and also separately within the previously defined bivariate TGS combination. Depicted Kaplan Meier strata reflect dichotomous strata for each gene relative to its median (A-D), and the TGS relative to pre-defined ternary thresholds from DLBCL1 (E,F).

REFERENCES

1. Cheson BD, Horning SJ, Coiffier B, et al. Report of an International Workshop to Standardize Response Criteria for Non-Hodgkin's Lymphomas. *J Clin Oncol* 1999;17:1244-.
2. Jaffe ES, World Health Organization. Pathology and genetics of tumours of haematopoietic and lymphoid tissues. Lyon, Oxford: IARC Press; Oxford University Press (distributor); 2001.
3. Lenz G, Wright G, Dave SS, et al. Stromal gene signatures in large-B-cell lymphomas. *N Engl J Med* 2008;359:2313-23.
4. Hummel M, Bentink S, Berger H, et al. A biologic definition of Burkitt's lymphoma from transcriptional and genomic profiling. *New England Journal of Medicine* 2006;354:2419.
5. Dai M, Wang P, Boyd A, et al. Evolving gene/transcript definitions significantly alter the interpretation of GeneChip data. *Nucleic acids research* 2005;33:e175.
6. Rosenwald A, Wright G, Chan WC, et al. The use of molecular profiling to predict survival after chemotherapy for diffuse large-B-cell lymphoma. *N Engl J Med* 2002;346:1937-47.
7. Wang Y, Klijn JGM, Zhang Y, et al. Gene-expression profiles to predict distant metastasis of lymph-node-negative primary breast cancer. *The Lancet* 2005;365:671-9.
8. Mizuno H, Kitada K, Nakai K, Sarai A. Prognoscan: a new database for meta-analysis of the prognostic value of genes. *BMC Medical Genomics* 2009;2:18.
9. Smith JJ, Deane NG, Wu F, et al. Experimentally Derived Metastasis Gene Expression Profile Predicts Recurrence and Death in Patients With Colon Cancer. *Gastroenterology* 2010;138:958-68.
10. Shedden K, Taylor JMG, Enkemann SA, et al. Gene expression-based survival prediction in lung adenocarcinoma: a multi-site, blinded validation study. *Nat Med* 2008;14:822-7.
11. Abel U, Berger J, Wiebelt H. CRITLEVEL: an exploratory procedure for the evaluation of quantitative prognostic factors. *Methods of information in medicine* 1984;23:154-6.
12. Miller R, Siegmund D. Maximally selected chi square statistics. *Biometrics* 1982;38:1011-6.
13. Pichler K, Kattan T, Gentsch J, et al. Strong induction of 4-1BB, a growth and survival promoting costimulatory receptor, in HTLV-1-infected cultured and patients' T cells by the viral Tax oncoprotein. *Blood* 2008;111:4741-51.

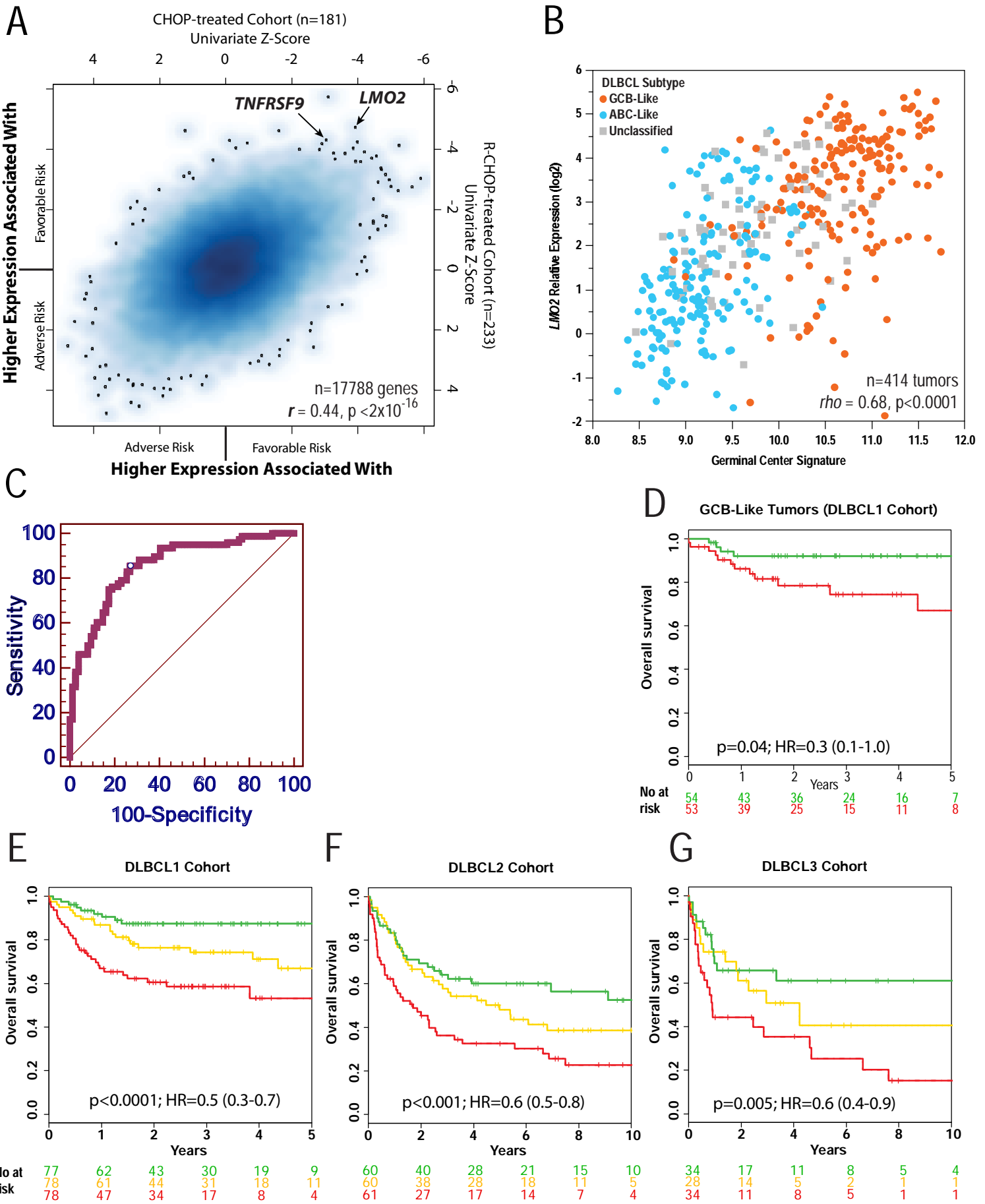


Figure S1

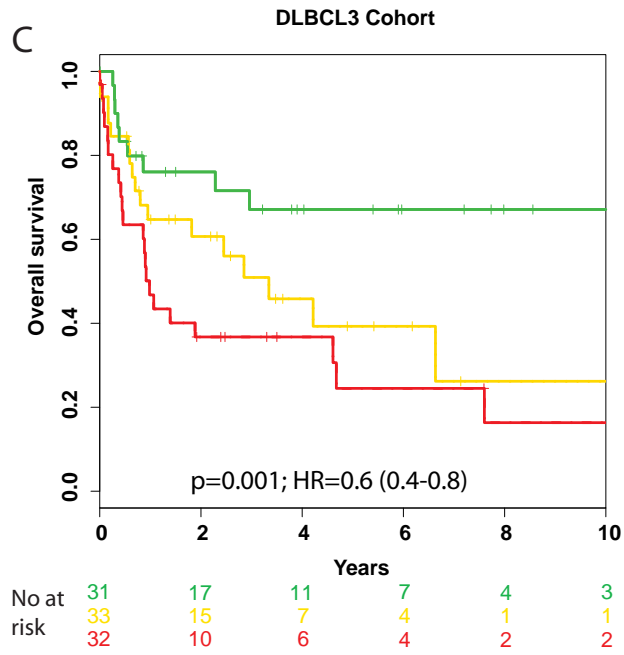
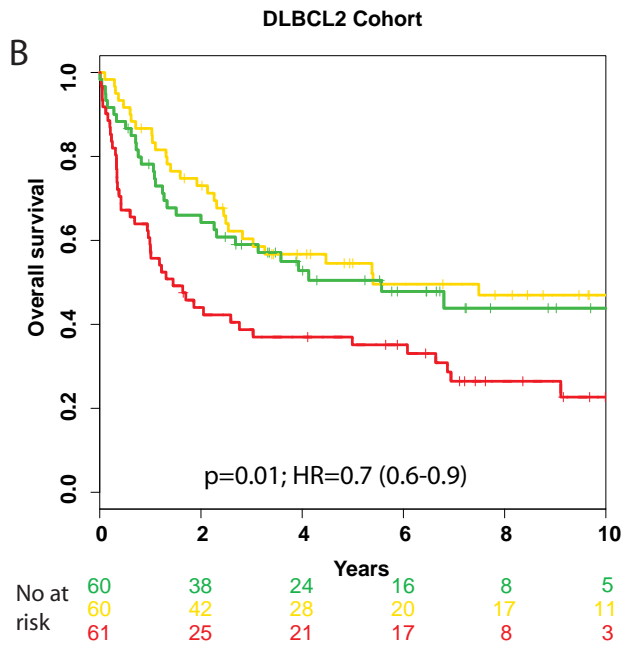
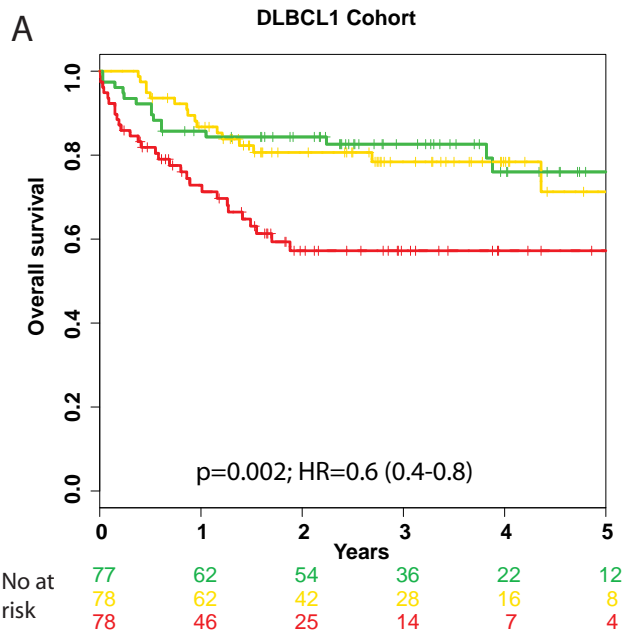
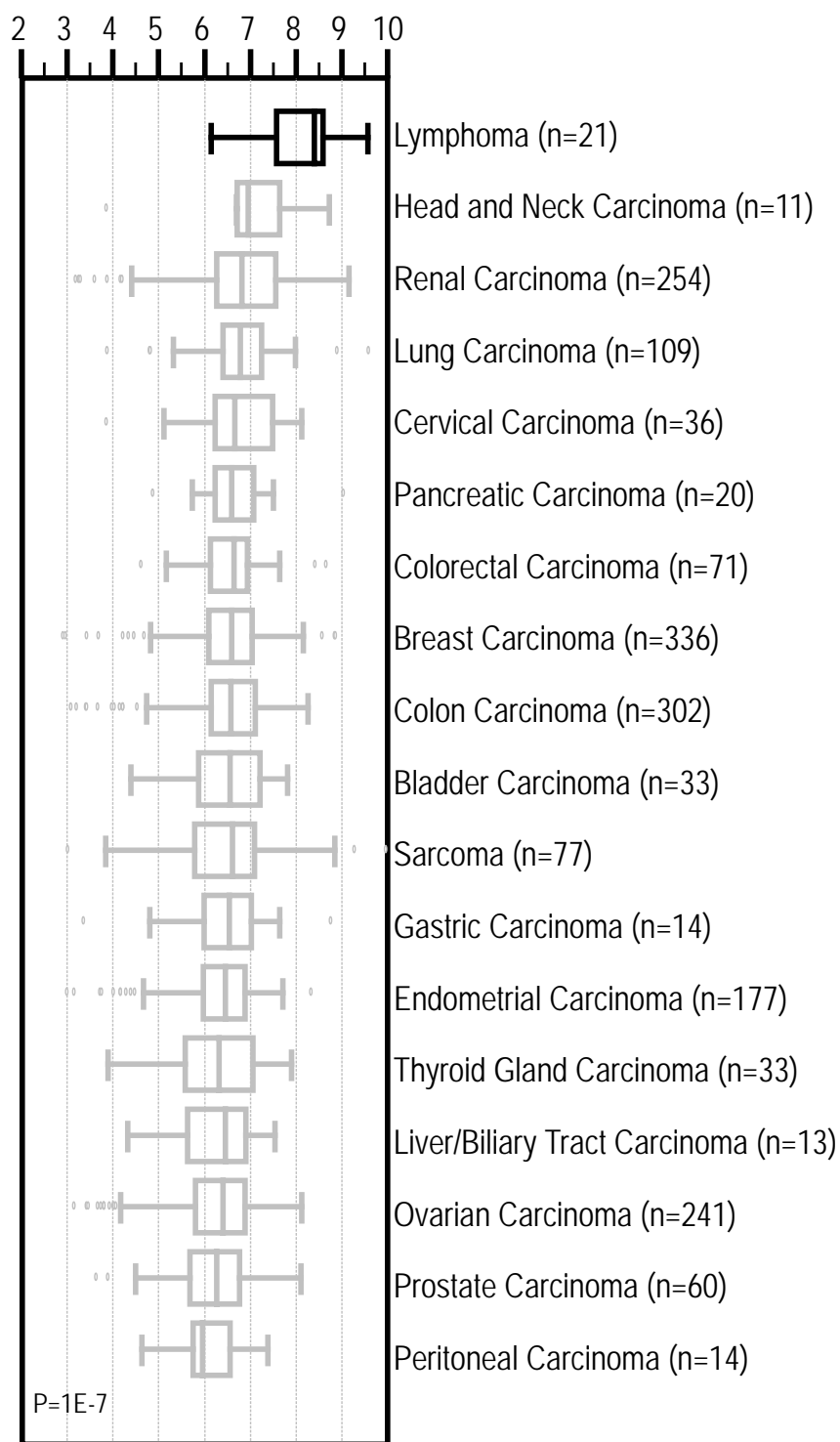
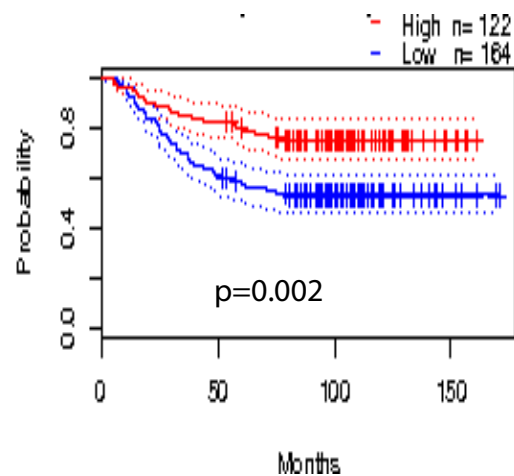


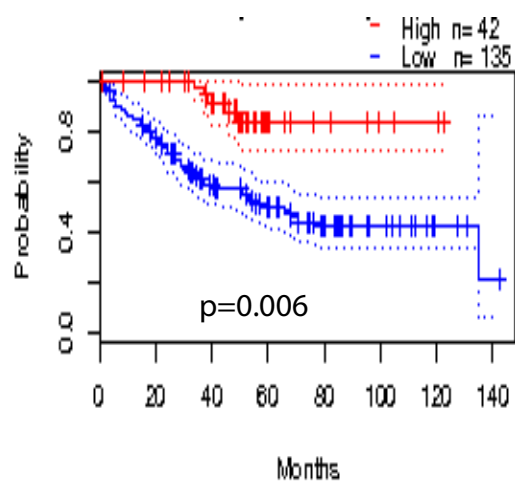
Figure S2

A*TNFRSF9* Relative Expression (log2)**B**

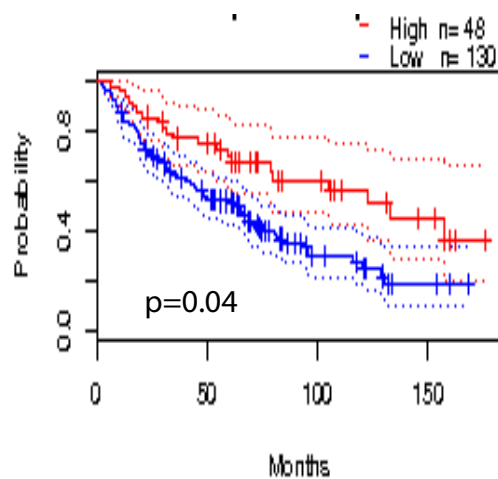
Breast Adenocarcinoma

TNFRSF9 Expression:**C**

Colorectal Adenocarcinoma

TNFRSF9 Expression:**D**

Lung Adenocarcinoma

TNFRSF9 Expression:

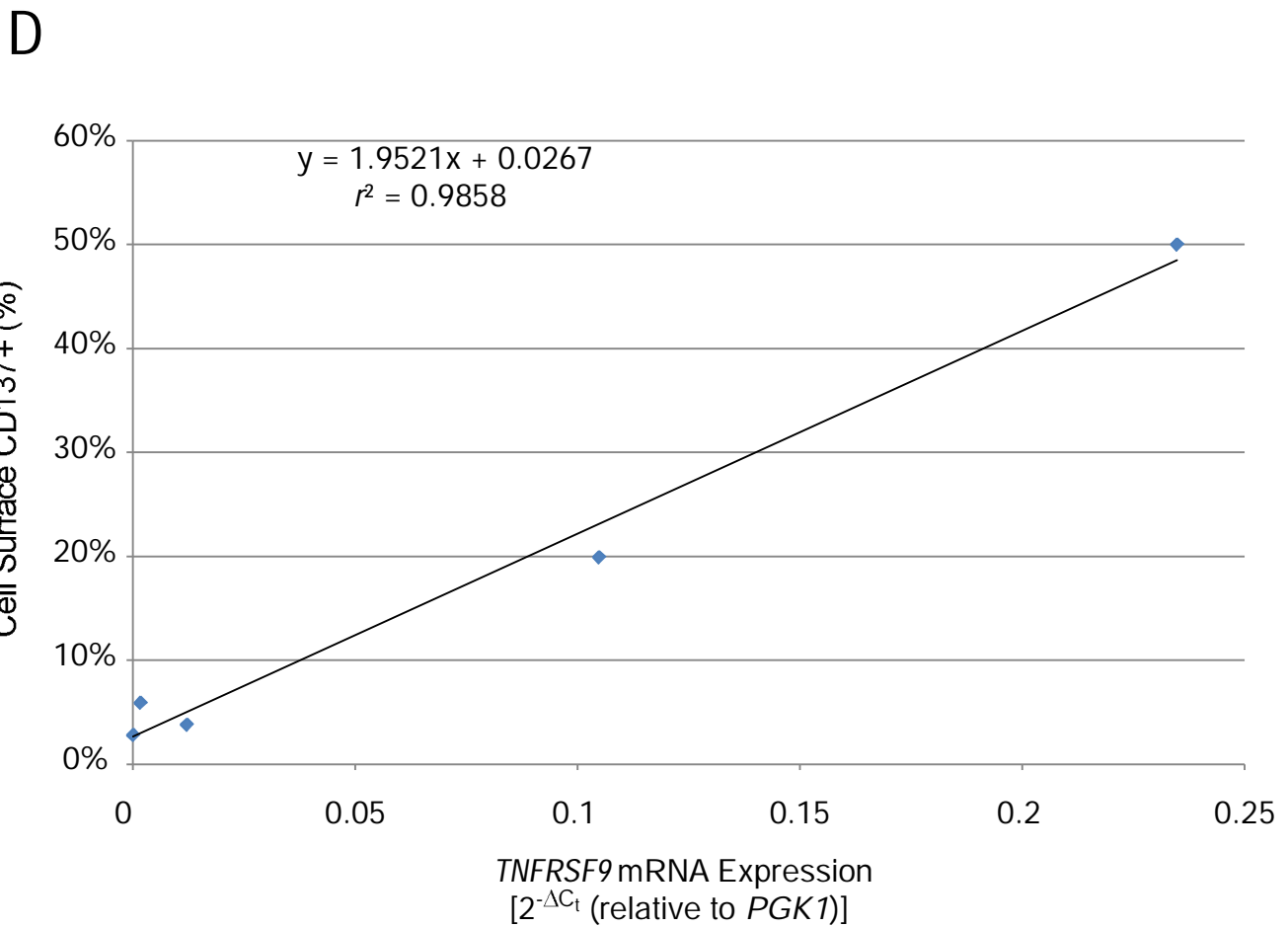
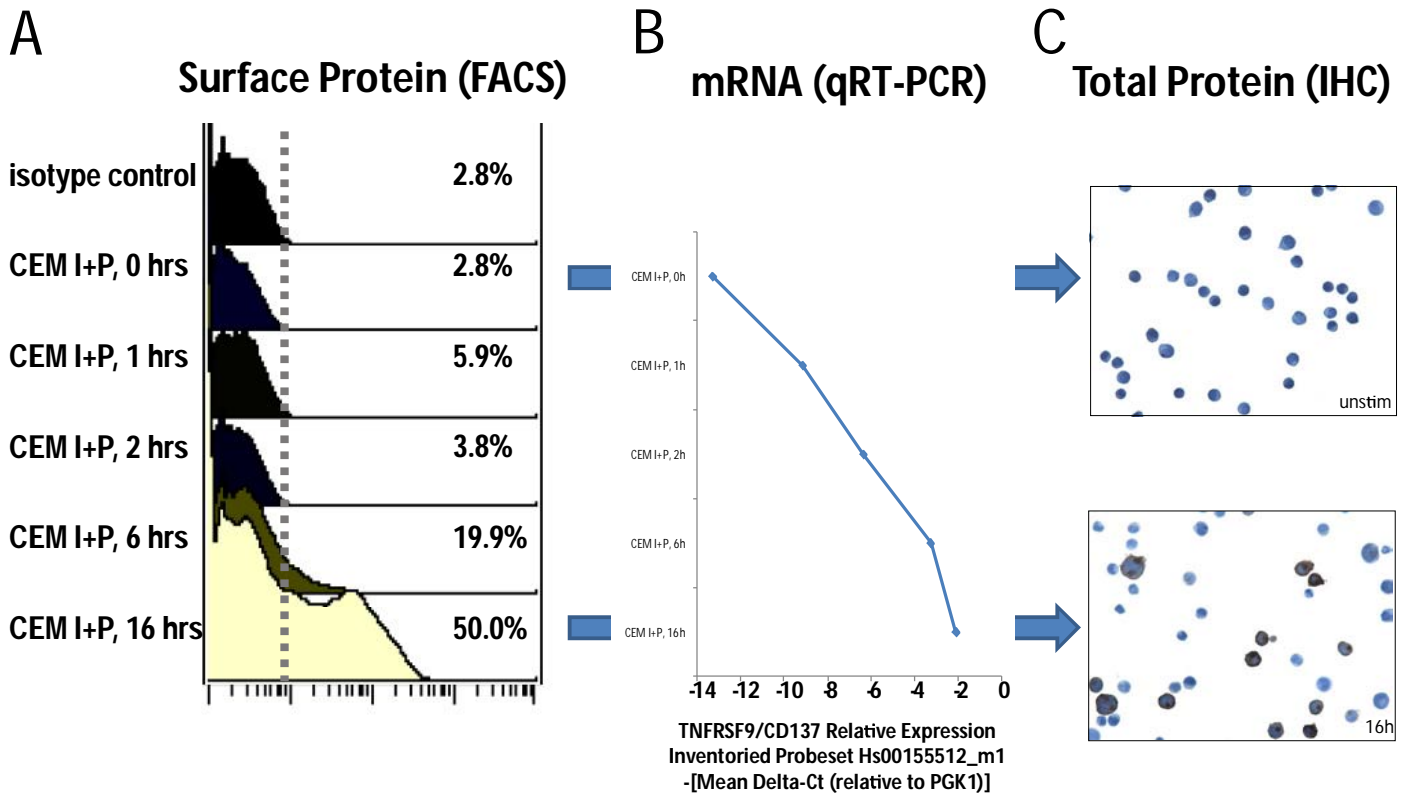


Figure S4

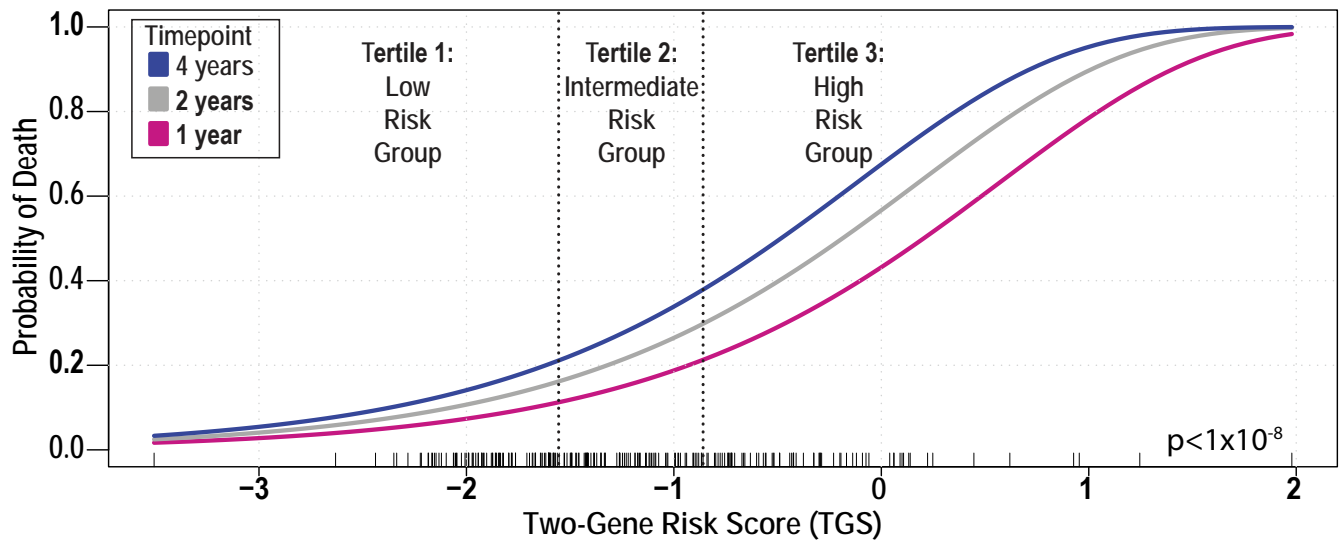


Figure S5

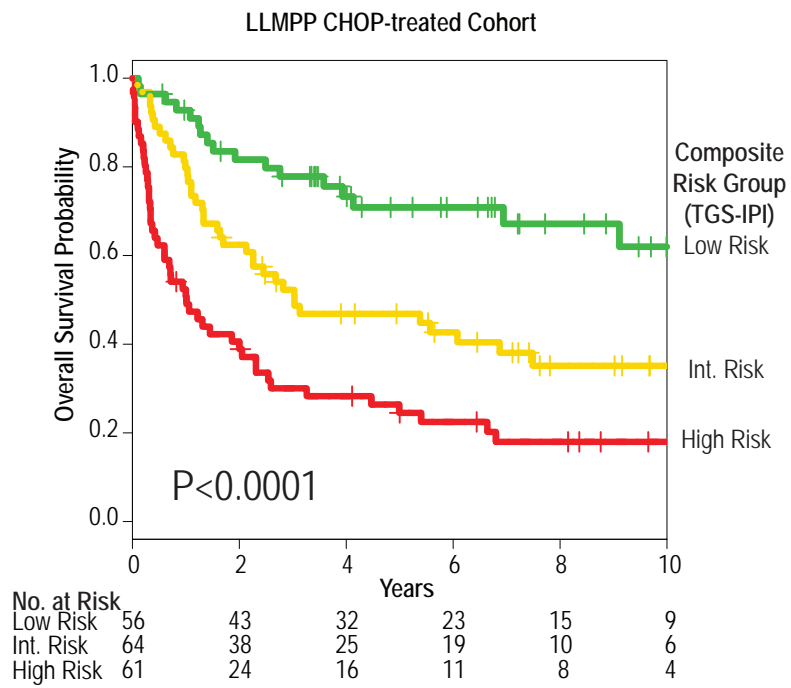


Figure S6

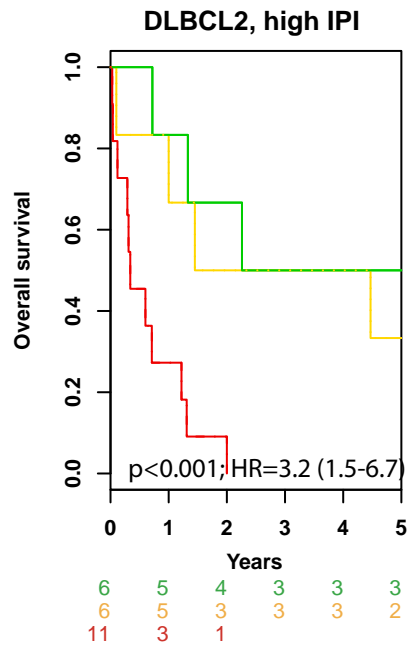
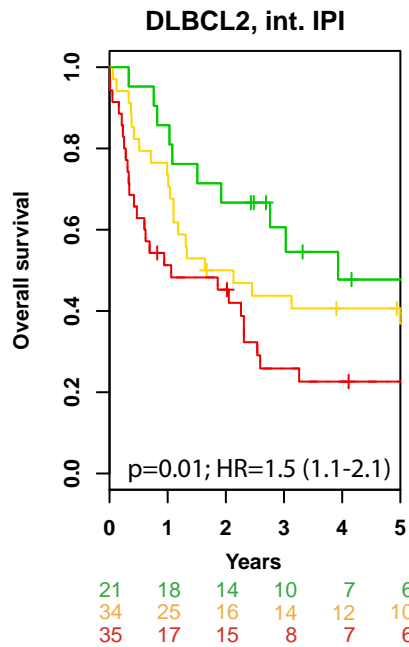
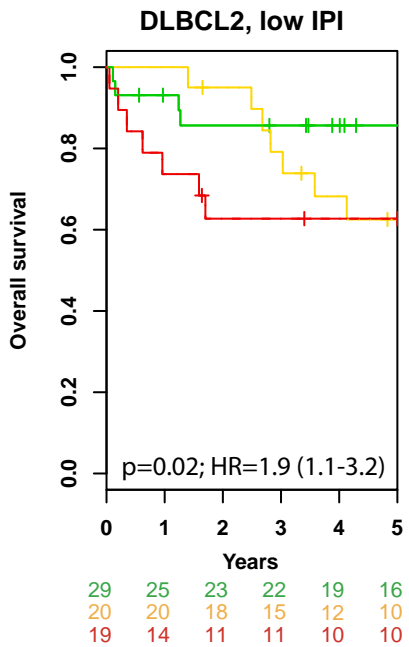
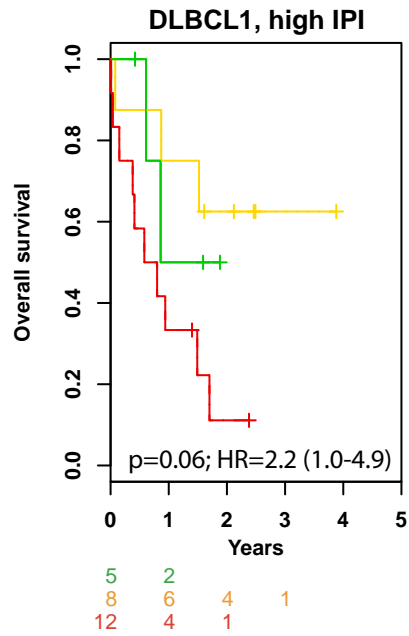
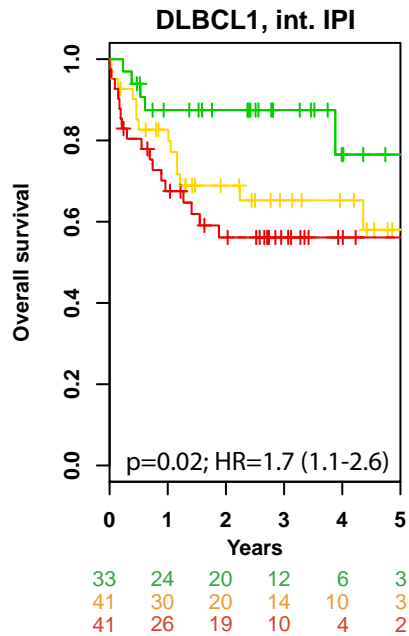
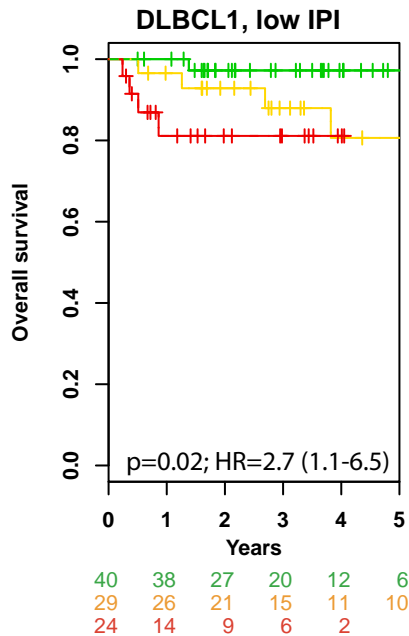
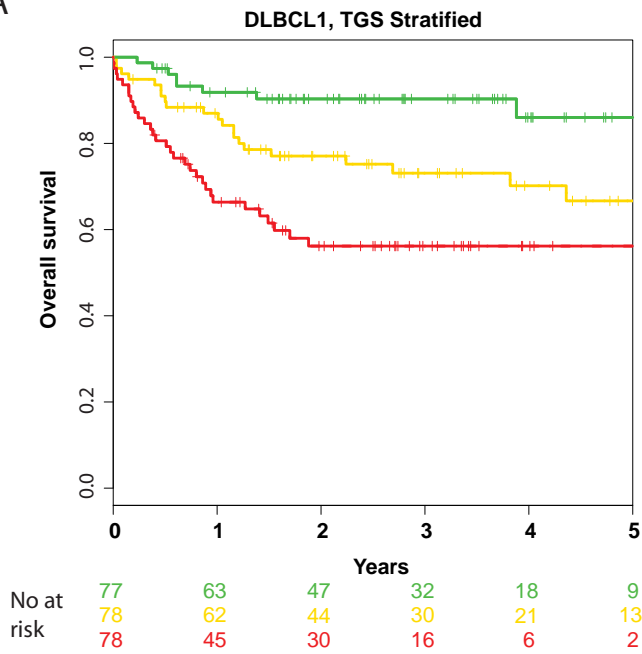
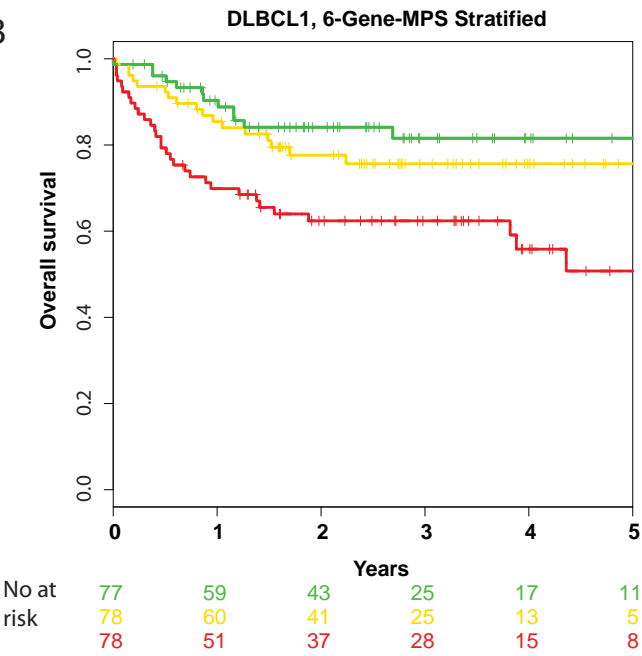


FIGURE S7

A



B



C

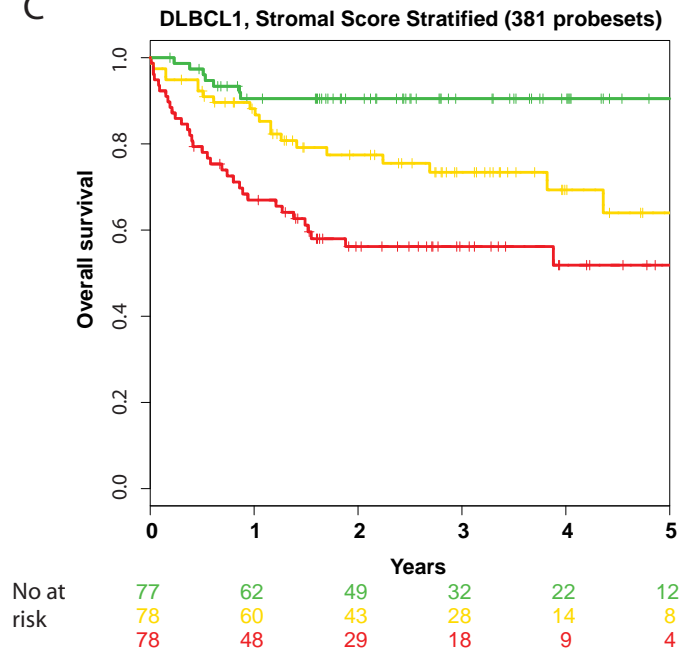


Figure S8

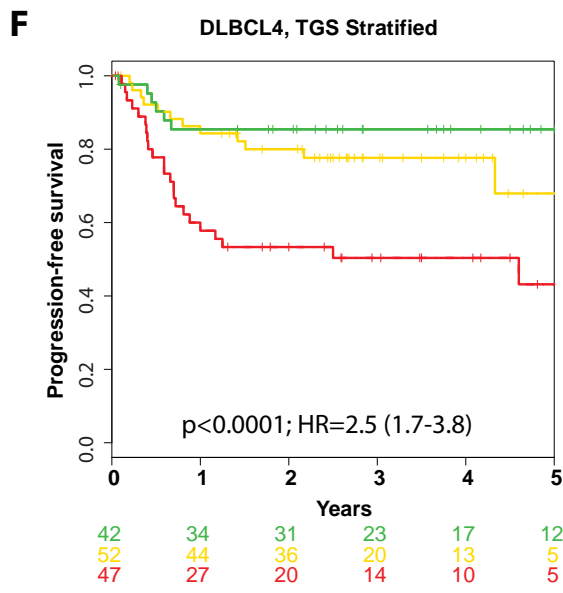
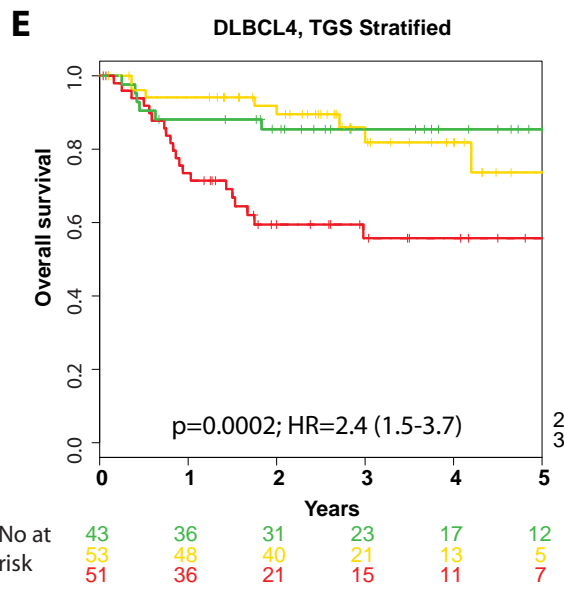
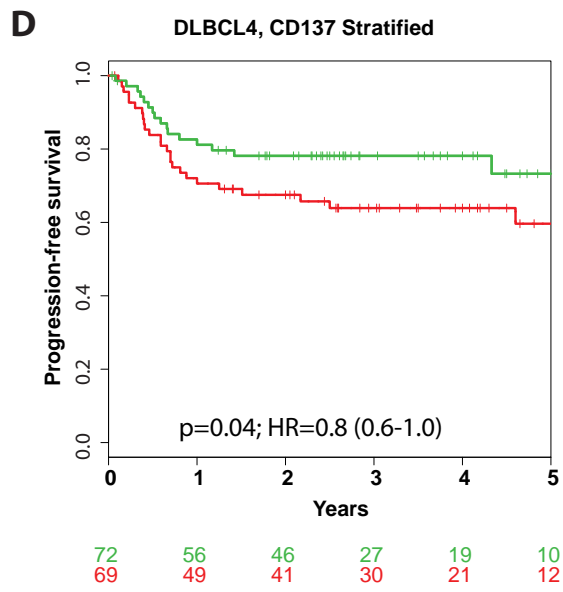
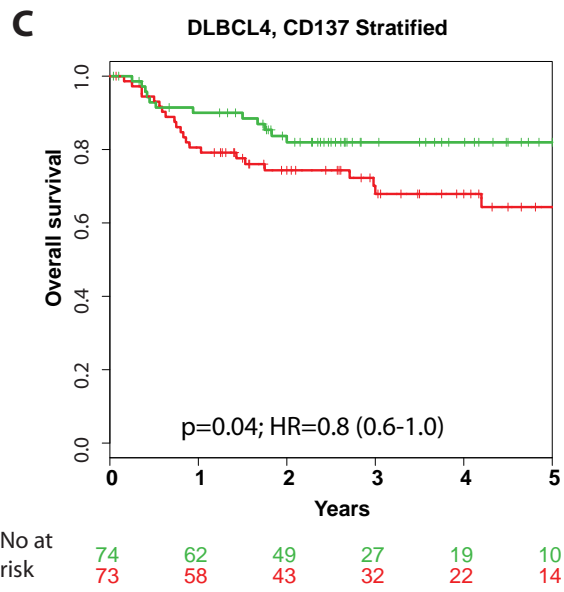
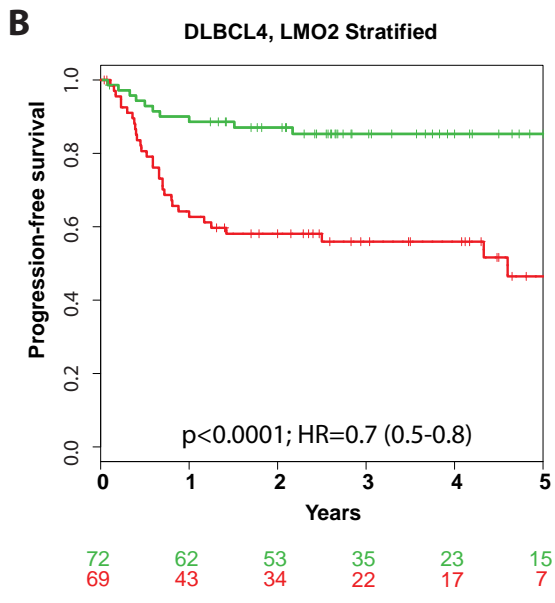
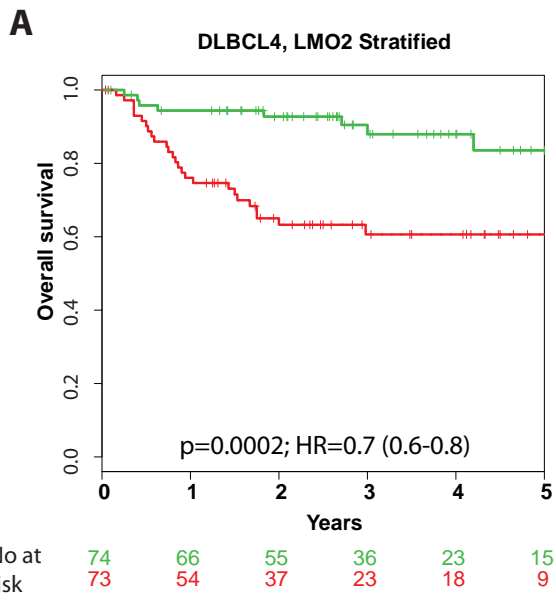


Figure S9